JACS
JOURNAL OF THE AMERICAN CHEMICAL SOCIETY

COMMUNICATION

pubs.acs.org/JACS

The Importance of Bulk Ti^{3+} Defects in the Oxygen Chemistry on Titania Surfaces

Estephania Lira, Stefan Wendt,* Peipei Huo, Jonas Ø. Hansen, Regine Streber, Søren Porsgaard, Yinying Wei, Ralf Bechstein, Erik Lægsgaard, and Flemming Besenbacher*

Interdisciplinary Nanoscience Center (iNANO) and Department of Physics and Astronomy, Aarhus University, DK 8000 Aarhus C, Denmark

Supporting Information

ABSTRACT: The role of bulk defects in the oxygen chemistry on reduced rutile $TiO_2(110)-(1 \times 1)$ has been studied by means of temperature-programmed desorption spectroscopy and scanning tunneling microscopy measurements. Following O_2 adsorption at 130 K, the amount of O_2 desorbing at ~410 K initially increased with increasing density of surface oxygen vacancies but decreased after further reduction of the $TiO_2(110)$ crystal. We explain these results by withdrawal of excess charge (Ti^{3+}) from the $TiO_2(110)$ lattice to oxygen species on the surface and by a reaction of Ti interstitials with O adatoms upon heating. Important consequences for the understanding of the O_2-TiO_2 interaction are discussed.

The interaction of oxygen with titania (TiO_2) is crucial in fields such as heterogeneous catalysis, photocatalysis, and gas sensing,[1−16] but the role of oxygen in these applications is still unclear.[3] To shed light on the O_2-TiO_2 interaction at the atomic scale, model studies of rutile $TiO_2(110)$ crystals under ultrahigh vacuum (UHV) have been performed.[1−3,8−13,17−27] Presently, the literature on the O_2-TiO_2 interaction is surprisingly heterogeneous, and various conflicting models have been proposed.[8,9,18−23] For example, at adsorption temperatures (T_{ad}) ≥ 400 K, the important role of Ti interstitials in the oxygen chemistry has been recognized;[8,11] however, for $T_{ad} \leq 300$ K, it has been proposed that surface defects control the oxygen chemistry on reduced rutile $TiO_2(110)$.[18−21]

The rutile $TiO_2(110)-(1 \times 1)$ surface consists of alternating rows of fivefold-coordinated Ti atoms and protruding, twofold-coordinated bridging oxygen atoms (O_{br}). The Ti atoms underneath the O_{br} atoms are sixfold-coordinated, as are the other Ti atoms in stoichiometric rutile. Ar^+-sputtered and vacuum-annealed $TiO_2(110)$ crystals are n-type semiconductors because of bulk defects such as Ti interstitials, O vacancies, and crystallographic shear planes.[8,9,11,13] The surfaces of vacuum-annealed $TiO_2(110)$ crystals are characterized by the presence of O_{br} vacancies (O_{br} vac.) and/or H adatoms (H_{ad}, often also denoted as OH_{br}).[8−10,17] This is different from anatase $TiO_2(101)$, for which scanning tunneling microscopy (STM) studies have revealed the absence of surface O vac. defects.[28]

It is generally accepted that adsorbed O_2 species acquire negative charge upon adsorption on TiO_2 surfaces.[1,2,8,13,18,21,29,30] Adsorbed oxygen species are capable of causing upward band bending, which is of great importance in many of the applications of TiO_2.[8,13,15,16] In most of the previous studies, an idealized model has been invoked in which O_2 molecules adsorb at O_{br} vac. sites and charge donation from other defects does not occur (Figure 1, model A).[18,19] Within model A, it has been proposed that the O_2 desorption peak at ~410 K[2,18,19,22] is associated with O_2 desorption from O_{br} vac. defects.[18,19] Recently, we proposed another model to explain the desorption of O_2 molecules at ~410 K.[22] Within this model, O_2 molecules and O adatoms (O_{ad}) are postulated to withdraw the charge primarily from the near-surface region (Figure 1, model B).[13,17,22,24] The desorption of O_2 molecules at ~410 K would then be caused by a depletion of the excess charge in the near-surface region that occurs when outdiffusing Ti interstitials react with the O_{ad} species on the surface.[22] The O_{ad} species appearing on the surface directly after O_2 exposure at 120−130 K result from O_2 dissociation reactions at O_{br} vac. defects (first channel).[13,17,22]

In this work, we utilized a combination of temperature-programmed desorption (TPD) and STM to explore further the $O_2-TiO_2(110)$ interaction and the role of defects. The O_2 TPD peak at ~410 K was monitored as a function of the $TiO_2(110)$ crystal reduction state, and the surface morphology before and after oxidation of the crystal was studied by high-resolution STM.

The TPD and STM experiments were carried out in a UHV chamber equipped with a quadrupole mass spectrometer (QMS), a home-built, variable-temperature Aarhus scanning tunneling microscope,[31] and standard facilities for sample preparation and characterization.[17,22] The differentially pumped QMS was connected to the chamber via a closed cone with a small aperture ($d \approx 3$ mm) facing the sample at a distance of 1 mm, ensuring that only molecules desorbing from the sample could reach the QMS filament. The sample temperature was measured using a K-type thermocouple spot-welded to the sample plate with the thermocouple in direct contact with the crystal. The $TiO_2(110)$ crystal was prepared by applying cycles of Ar^+ sputtering (1 kV, ~1 nA, 8 min) and vacuum annealing (20 min). Initially, the crystal was annealed at 850 K, but in the course of ~80 preparation cycles, the annealing temperature was gradually increased to a final value of 960 K. Oxygen exposures are given in langmuirs ($1\ L = 1.33 \times 10^{-6}$ mbar·s), and the defect densities are given in % monolayers (% ML), where 1 ML is the density of the (1×1) unit cell ($5.2 \times 10^{14}\ cm^{-2}$).

Figure 2 shows O_2 TPD spectra obtained for (i) a clean, reduced $TiO_2(110)$ surface with O_{br} vac. defects (r-TiO_2) and (ii) a $TiO_2(110)$ surface with H_{ad} species (h-TiO_2). On h-TiO_2, no O_{br} vac. persisted, as all of them were healed via water

Received: January 28, 2011
Published: April 11, 2011

dx.doi.org/10.1021/ja200884w | J. Am. Chem. Soc. 2011, 133, 6529–6532

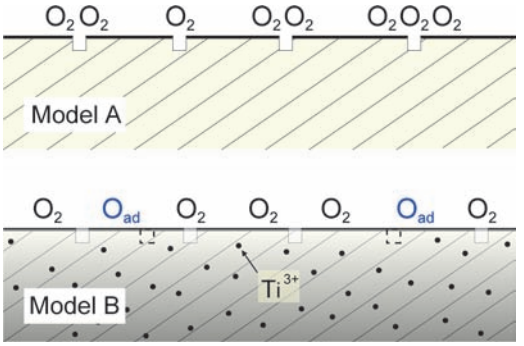

Figure 1. Schematic diagram illustrating two models for O_2 adsorption on reduced $TiO_2(110)$ at ~130 K. Model A: purely O vac.-assisted adsorption. Model B: O_2 adsorption enabled predominantly through charge withdrawal from Ti^{3+} defects in the near-surface region.

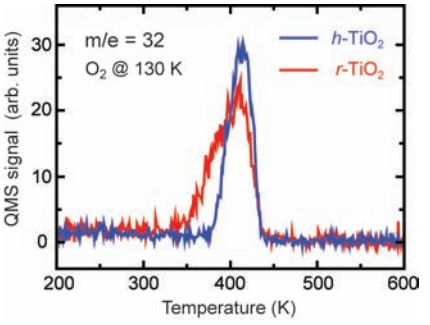

Figure 2. O_2 TPD spectra (heating rate = 2 K/s) obtained for *r*- and *h*-TiO_2 using 20 L O_2 (saturation). A medium-reduced, vacuum-annealed $TiO_2(110)$ crystal was used in both experiments.

dissociation reactions.[9,17,24] Both experiments were conducted with a medium-reduced $TiO_2(110)$ crystal, and in each case, the clean surface had O_{br} vac. densities of ~8% ML. Following 20 L O_2 exposure at 130 K, the amounts of O_2 desorbed from *r*- and *h*-TiO_2 between 350 and 450 K were very similar, in agreement with previous results.[20] As revealed in Figure 2, the line shapes of the two O_2 TPD spectra differed somewhat, with the O_2 molecules being slightly more stabilized on *h*-TiO_2. All of the charge-donating defects (O_{br} vac., H_{ad}, and bulk-defects such as Ti interstitials) may contribute to the stabilization of O_2 molecules on the surface.[29,30,32] Therefore, solely on the basis of the O_2 TPD spectra displayed in Figure 2, it cannot be deduced which defects are the most relevant ones.

Figure 3 shows the O_2 TPD peak areas found in a series of O_2 TPD experiments that were conducted using the same sample but with the crystal in different reduction states. In order to provide a measure of the bulk-reduction state, we determined the O_{br} vac. densities by means of STM measurements on the corresponding *r*-$TiO_2(110)$ surfaces before the TPD experiments were performed (see the Supporting Information). In the TPD experiments, both *r*- and *h*-$TiO_2(110)$ surfaces were studied, and all of the surfaces were saturated with O_2 at 130 K. The O_2 TPD peak areas can be compared for *r*- and *h*-$TiO_2(110)$ surfaces because equal amounts of O_2 desorb from the surface provided that the bulk reduction of the crystals and T_{ad} are similar (cf. Figure 2). As shown in Figure 3, the amount of desorbing O_2 increased between 6 and 8% ML O_{br} vac. density, and a maximum was observed at ~8.3% ML. Surprisingly, with

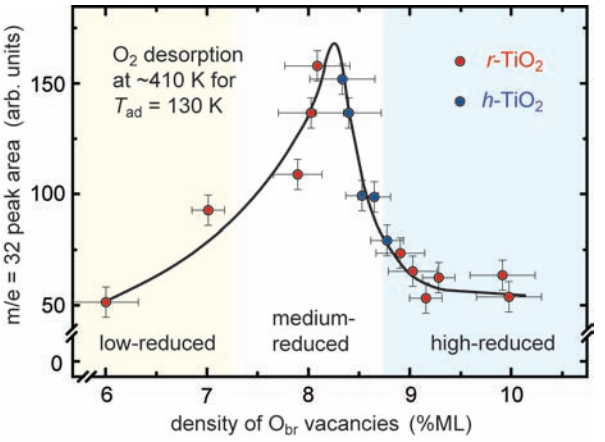

Figure 3. O_2 TPD peak area as a function of the crystal reduction state. The density of O_{br} vac. defects on the terraces (estimated from corresponding STM analysis; see the Supporting Information) was taken as a measure of the bulk-reduction state. O_2 was dosed at 130 K onto *r*- and *h*-TiO_2 surfaces, respectively. In all cases, at least 20 L was dosed to saturate the crystal surface with oxygen species. The plot is based on O_2 TPD spectra that were all collected from the same $TiO_2(110)-(1 \times 1)$ crystal.

further reduction of the crystal, the amount of desorbing O_2 declined significantly. This is a remarkable result that is difficult to explain within model A. If O_2 were stabilized on the surface exclusively through charge withdrawal from surface defects (O_{br} vac. and H_{ad}), the amount of desorbing O_2 would be directly proportional to the density of these defects, which was not the case. However, the decline of the O_2 TPD peak area for higher crystal reduction states (i.e., O_{br} vac. densities higher than ~8.3% ML) can be rationalized within model B, as will be discussed below.

On low-reduced $TiO_2(110)$ crystals, only a small amount of O_2 is adsorbed (i.e., the amount of desorbing O_2 at ~410 K is limited by the adsorption at 130 K). With increasing bulk reduction of the $TiO_2(110)$ crystal, more excess charge is available on the surface, and thus, more O_2 adsorbs at 130 K. As a result, the O_2 TPD peak at ~410 K increases initially for O_{br} vac. densities between 6 and 8% ML. It should be noted, however, that a substantial amount of O_2 can be lost upon heating of the crystal through O_2 dissociation reactions.[22,23] Recent STM studies revealed the existence of a non-vacancy-assisted O_2 dissociation channel that leads to the formation of paired O_{ad} in the Ti troughs (second channel).[9,13,22,23] On low- and medium-reduced $TiO_2(110)$ crystals, this second O_2 dissociation channel sets in between 150 and 180 K.[22]

The amount of desorbing O_2 at ~410 K is high when two conditions are fulfilled: (i) O_2 adsorption at 130 K is sufficiently high, and (ii) only a small amount of O_2 is lost via O_2 dissociation upon heating of the crystal. In the course of the TPD experiments, O_2 molecules first dissociate in the Ti troughs and residual O_{br} vac. sites, leading to the formation of additional O_{ad}. At ~360 K, the Ti interstitials in the near-surface region begin to diffuse toward the surface, where they react with O_{ad} species.[23] In this way, small TiO_x islands with $x \approx 2$ are formed on the terraces.[13,22,23] Simultaneously, the residual intact O_2 molecules begin to desorb from the surface because the Ti^{3+} excess charge in the near-surface region is depleted.[22] On the more-reduced $TiO_2(110)$ crystals, more Ti^{3+} excess charge is available in the bulk and the near-surface region. As a result, the dissociation of O_2 molecules in the Ti troughs

dx.doi.org/10.1021/ja200884w | J. Am. Chem. Soc. 2011, 133, 6529–6532

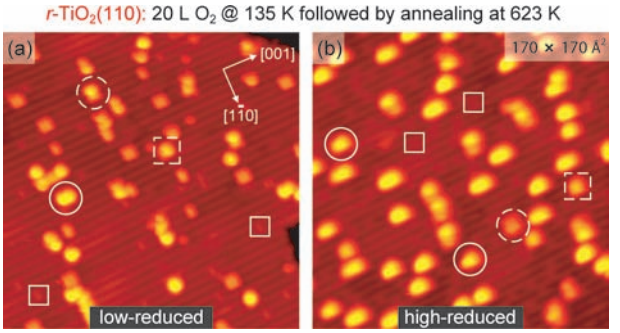

Figure 4. STM images (constant-current mode, tunneling voltage ≈ +1.25 V, tunneling current ≈ 0.1 nA) obtained after 20 L O_2 exposure at 135 K followed by annealing at 623 K for 120 s for (a) a low-reduced $TiO_2(110)$ crystal and (b) a high-reduced crystal. The O_{br} vac. densities on the terraces before O_2 exposure were (a) ∼3.5 and (b) ∼10.0% ML. Symbols indicate O_{br} vac. (solid-line squares) and TiO_x islands of identical sizes (dashed-line squares, solid-line circles, and dashed-line circles).

(second channel) is hindered by only a low energy barrier, as revealed by means of density functional theory calculations.[13,30] This explains why the second O_2 dissociation channel opens at lower temperature on medium-reduced crystals than on low-reduced ones.[22] For high-reduced $TiO_2(110)$ crystals, we expect an increase in the O_2 dissociation rate upon heating of the crystal because the density of charge donors is even higher than for medium-reduced crystals. Directly after saturation of high-reduced $TiO_2(110)$ crystals with O_2 at 130 K, the density of O_{ad} was ∼8% ML (not shown). A substantial portion of the Ti^{3+} excess charge in the near-surface region may have been depleted as a result of the adsorption of these O_{ad}.[21,22] Since O_2 and O_{ad} compete for the available Ti^{3+} excess charge,[21,22] we speculate that the initial O_2 coverage on high-reduced $TiO_2(110)$ crystals is only slightly larger than that on medium-reduced $TiO_2(110)$ crystals. When high-reduced $TiO_2(110)$ crystals are heated, many more oxygen species can react with the Ti interstitials than in the case of less-reduced samples, which explains the decline of the O_2 TPD peak area with increasing crystal reduction (cf. Figure 3).

The STM images displayed in Figure 4 directly show that the amount of oxygen incorporation into the crystal depends on the reduction state of the $TiO_2(110)$ crystal (i.e., on the available Ti^{3+} excess charge). Following the 20 L O_2 exposure at 135 K and annealing at 620 K for 120 s, TiO_x islands (with similar densities) appeared on the surface in both experiments. However, the average size of the TiO_x islands was much smaller for the low-reduced crystal (Figure 4a) than on the high-reduced crystal (Figure 4b), indicating that more O_2 reacted with the high-reduced crystal. It should be noted that the bulk of high-reduced $TiO_2(110)$ crystals constitutes a reservoir of Ti interstitials and possible other bulk defects in which the number of such species is much higher than the number of adsorption sites on the surface. The STM data presented in Figure 4 support the scheme described above, explaining why only a small amount of O_2 desorbs at ∼410 K from the high-reduced $TiO_2(110)$ crystals.

The results presented here reveal that model B in Figure 1 describes the O_2-TiO_2 interaction more completely than model A, indicating that the oxygen chemistry on reduced $TiO_2(110)$ is governed by bulk defects. While the latter is apparent for $T_{ad} \geq 360$ K,[8,11,23] the strong influence of charge-donating bulk defects is less obvious for $T_{ad} < 360$ K because the diffusion of Ti interstitials is kinetically hindered at these temperatures.[23] However, the bulk Ti^{3+} defects such as Ti interstitials are also essential for $T_{ad} < 360$ K because these defects provide most of the charge (very probably more than 90%)[22] that is required for the adsorption of O_2 and O_{ad} species. The presented results indicate that Ti^{3+} excess charge can easily be withdrawn by the adsorbates on the surface from deeper layers of the $TiO_2(110)$ crystal, even at 130 K. This conclusion is consistent with transport[33] and thin-film growth[34] studies as well as with electron paramagnetic resonance spectroscopy studies addressing TiO_2-based materials for applications in photocatalysis.[4−7] Such an ionosorption model may reconcile previously published experimental data on rutile $TiO_2(110)$ obtained at low and high T_{ad} as well as numerous data obtained in the fields of materials science and surface science. The insight gained for rutile $TiO_2(110)$ crystals may also be applicable to anatase TiO_2 and other reducible oxides such as SnO_2 and ZnO.

■ ASSOCIATED CONTENT

Supporting Information. Background literature summary, experimental details, and additional STM data. This material is available free of charge via the Internet at http://pubs.acs.org.

■ AUTHOR INFORMATION

Corresponding Author
swendt@phys.au.dk; fbe@inano.au.dk

■ ACKNOWLEDGMENT

We acknowledge the support of iNANO by the Danish Research Agency, the Strategic Research Council, the Villum Kahn Rasmussen Foundation, the Carlsberg Foundation, and the European Research Council through an Advanced ERC Grant (F.B.). We are grateful to J. T. Yates, Jr., and B. Hammer for stimulating discussions.

■ REFERENCES

(1) Thompson, T. L.; Yates, J. T., Jr. *Chem. Rev.* **2006**, *106*, 4428–4453.
(2) Thompson, T. L.; Yates, J. T., Jr. *Top. Catal.* **2005**, *35*, 197–210.
(3) Fujishima, A.; Zhang, X. T.; Tryk, D. A. *Surf. Sci. Rep.* **2008**, *63*, 515–582.
(4) Aono, M.; Hasiguti, R. R. *Phys. Rev. B* **1993**, *48*, 12406–12414.
(5) Attwood, A. L.; Murphy, D. M.; Edwards, J. L.; Egerton, T. A.; Harrison, R. W. *Res. Chem. Intermed.* **2003**, *29*, 449–465.
(6) Gopal, N. O.; Lo, H. H.; Sheu, S. C.; Ke, S. C. *J. Am. Chem. Soc.* **2010**, *132*, 10982–10983.
(7) Zuo, F.; Wang, L.; Wu, T.; Zhang, Z. Y.; Borchardt, D.; Feng, P. Y. *J. Am. Chem. Soc.* **2010**, *132*, 11856–11857.
(8) Diebold, U. *Surf. Sci. Rep.* **2003**, *48*, 53–229.
(9) Dohnálek, Z.; Lyubinetsky, I.; Rousseau, R. *Prog. Surf. Sci.* **2010**, *85*, 161–205.
(10) Pang, C. L.; Lindsay, R.; Thornton, G. *Chem. Soc. Rev.* **2008**, *37*, 2328–2353.
(11) Bowker, M.; Bennett, R. A. *J. Phys.: Condens. Matter* **2009**, *21* No. 474224.
(12) Valden, M.; Lai, X.; Goodman, D. W. *Science* **1998**, *281*, 1647–1650.
(13) Wendt, S.; Sprunger, P. T.; Lira, E.; Madsen, G. K. H.; Li, Z. S.; Hansen, J. Ø.; Matthiesen, J.; Blekinge-Rasmussen, A.; Lægsgaard, E.; Hammer, B.; Besenbacher, F. *Science* **2008**, *320*, 1755–1759.
(14) Benz, L.; Haubrich, J.; Quiller, R. G.; Jensen, S. C.; Friend, C. M. *J. Am. Chem. Soc.* **2009**, *131*, 15026–15031.

(15) Zhang, Z.; Yates, J. T., Jr. *J. Am. Chem. Soc.* **2010**, *132*, 12804–12807.
(16) Porsgaard, S.; Jiang, P.; Borondics, F.; Wendt, S.; Liu, Z.; Bluhm, H.; Besenbacher, F.; Salmeron, M. *Angew. Chem.* **2011**, *123*, 2314–2317.
(17) Wendt, S.; Schaub, R.; Matthiesen, J.; Vestergaard, E. K.; Wahlström, E.; Rasmussen, M. D.; Thostrup, P.; Molina, L. M.; Lægsgaard, E.; Stensgaard, I.; Hammer, B.; Besenbacher, F. *Surf. Sci.* **2005**, *598*, 226–245.
(18) Henderson, M. A.; Epling, W. S.; Perkins, C. L.; Peden, C. H. F.; Diebold, U. *J. Phys. Chem. B* **1999**, *103*, 5328–5337.
(19) Kimmel, G. A.; Petrik, N. G. *Phys. Rev. Lett.* **2008**, *100*, No. 196102.
(20) Petrik, N. G.; Zhang, Z. R.; Du, Y. G.; Dohnálek, Z.; Lyubinetsky, I.; Kimmel, G. A. *J. Phys. Chem. C* **2009**, *113*, 12407–12411.
(21) Petrik, N. G.; Kimmel, G. A. *J. Phys. Chem. C* **2011**, *115*, 152–164.
(22) Lira, E.; Hansen, J. Ø.; Huo, P.; Bechstein, R.; Galliker, P.; Lægsgaard, E.; Hammer, B.; Wendt, S.; Besenbacher, F. *Surf. Sci.* **2010**, *604*, 1945–1960.
(23) Zhang, Z.; Lee, J.; Yates, J. T., Jr.; Bechstein, R.; Lira, E.; Hansen, J. Ø.; Wendt, S.; Besenbacher, F. *J. Phys. Chem. C* **2010**, *114*, 3059–3062.
(24) Matthiesen, J.; Wendt, S.; Hansen, J. Ø.; Madsen, G. K. H.; Lira, E.; Galliker, P.; Vestergaard, E. K.; Schaub, R.; Lægsgaard, E.; Hammer, B.; Besenbacher, F. *ACS Nano* **2009**, *3*, 517–526.
(25) Scheiber, P.; Riss, A.; Schmid, M.; Varga, P.; Diebold, U. *Phys. Rev. Lett.* **2010**, *105*, No. 216101.
(26) Wang, Z.-T.; Du, Y. G.; Dohnálek, Z.; Lyubinetsky, I. *J. Phys. Chem. Lett.* **2010**, *1*, 3524–3529.
(27) Tan, S.; Ji, Y.; Zhao, Y.; Zhao, A.; Wang, B.; Yang, J.; Hou, J. G. *J. Am. Chem. Soc.* **2011**, *133*, 2002–2009.
(28) He, Y. B.; Dulub, O.; Cheng, H. Z.; Selloni, A.; Diebold, U. *Phys. Rev. Lett.* **2009**, *102*, No. 106105.
(29) Liu, L. M.; McAllister, B.; Ye, H. Q.; Hu, P. *J. Am. Chem. Soc.* **2006**, *128*, 4017–4022.
(30) Deskins, N. A.; Rousseau, R.; Dupuis, M. *J. Phys. Chem. C* **2010**, *114*, 5891–5897.
(31) Lauritsen, J. V.; Besenbacher, F. *Adv. Catal.* **2006**, *50*, 97–147.
(32) Stausholm-Møller, J.; Kristoffersen, H. H.; Hinnemann, B.; Madsen, G. K. H.; Hammer, B. *J. Chem. Phys.* **2010**, *133*, No. 144708.
(33) Yagi, E.; Hasiguti, R. R.; Aono, M. *Phys. Rev. B* **1996**, *54*, 7945–7956.
(34) Chambers, S. A.; Cheung, S. A.; Shutthanandan, V.; Thevuthasan, S.; Bowman, M. K.; Joly, A. G. *Chem. Phys.* **2007**, *339*, 27–35.